



## Advances in Nanocatalysis Research for Carbon Nanotubes Formation and Photocatalytic Degradation of Phenol

Abdul Rahman Mohamed \*, Minoo Tasbihi, Siang-Piao Chai

*School of Chemical Engineering, Engineering Campus, Universiti Sains Malaysia, Seri Ampangan, 14300 Nibong Tebal, S.P.S. Pulau Pinang, Malaysia*

Selected paper from Congress and Symposium of MKICS 2007 (18-19 April 2007)

### Introduction

Catalysts daily accelerate and boost thousands of different chemical reactions, and thereby form the basis for the multibillion dollar chemical industry worldwide and indispensable environmental protective technologies. Research in nanotechnology and nanoscience is expected to have a great impact on the development of new catalysts. The detailed understanding of chemistry of nanostructures and the ability to control materials on the nanometer scale will ensure a rational and cost-efficient development of new and more capable catalysts for a chemical process.

Recently, countries in Asia are setting up nanotechnology initiatives. Some of the major initial advances are expected to come in areas of increasing rates of reaction using nanocatalysts in catalytic processes. Although most production by catalysis is performed in large-scale reactors, the reaction that actually takes place in the catalyst occurs on the surface of highly dispersed metallic particles with typical dimensions of 1 – 100 nm (Fig. 1). Catalysts are perhaps the first industrial nanotechnology. It is well known that the catalytic activity of supported metal catalysts is strongly dependent on the size and shape of the metal particles. Nanoparticle catalysts are highly active since most of the particle surfaces can be available to catalysis. Many of the nanocatalysts have found applications in ammonia synthesis, environmental protection, photocatalysis, waste removal, fiber and mechanical industries.

Catalysis can play two principal roles in nanoscience, including (1) catalysts can be involved in some methods for preparing nanomaterials such as nanotubes; (2) some nanostructures themselves can serve as catalysts for additional chemical reactions. Both nanocatalysis aspects are highlighted in this paper, covering the topics of the use of nanocatalyst for photocatalytic degradation of phenol and methane decomposition into carbon nanotubes (CNTs).

### 1. Formation of CNTs via catalytic decomposition of methane

Carbon nanotubes (CNTs), demonstrating unique structural, mechanical, and electrical properties [1], possess many new important applications such as the quantum wires, field-effect transistors, field emitters, diodes, gas sensor, electric power storage, targeted drug delivery, catalyst support, reinforcing elements in composites, etc. [2-4]. This section highlights the tailor-making of CNTs with desirable morphologies through manipulating the nano-active metals and support of a catalyst.

Fig. 2 shows the TEM images of NiO/SiO<sub>2</sub> and NiO/Al<sub>2</sub>O<sub>3</sub> catalysts prepared via conventional impregnation method. The dark spots are NiO crystallites (indicated by arrows), and the shallow matters around these crystallites are assigned to the catalyst supports. It can be noted that NiO supported on SiO<sub>2</sub> is of larger size. Apparently, very

\* Corresponding Author.

E-mail address: [chrahman@eng.usm.my](mailto:chrahman@eng.usm.my) (Abdul Rahman Mohamed)

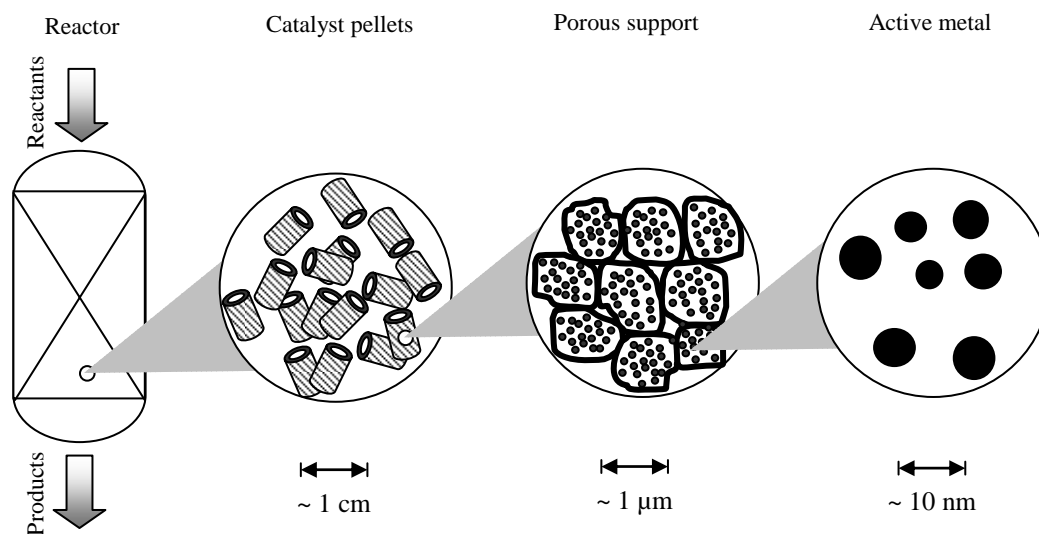
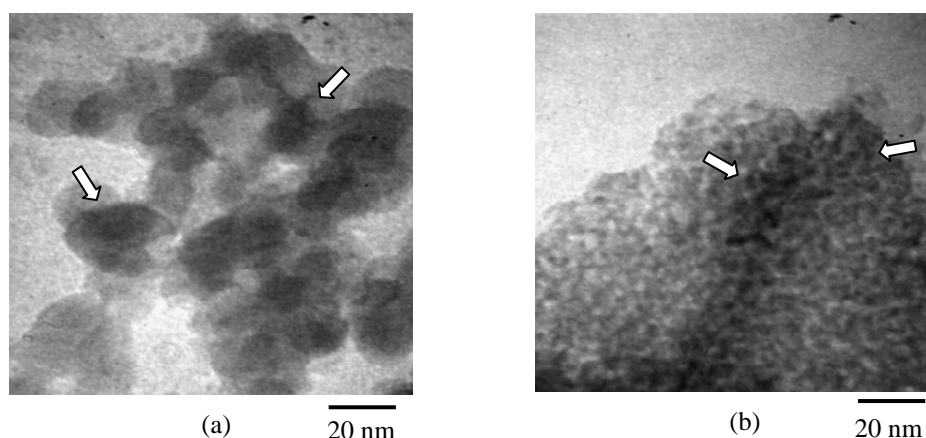


Fig.

1. Sche-



**Fig. 2.** TEM images of catalysts. (a) NiO/SiO<sub>2</sub> and (b) NiO/Al<sub>2</sub>O<sub>3</sub> [5]

small size NiO crystallites are formed on Al<sub>2</sub>O<sub>3</sub> support. The formation of smaller size NiO crystallites on alumina support is because of NiO/Al<sub>2</sub>O<sub>3</sub> catalyst possesses stronger metal-support interaction (MSI) effect. This helps in the dispersion of NiO crystallites, preventing their agglomeration to form larger cluster. On the contrary, NiO crystallites of larger size are formed on silica support. This is due to the lower MSI of NiO/SiO<sub>2</sub> catalyst [5]. This finding shows that the size of the active metals can be controlled by doping them on different catalyst supports [6,7].

Fig. 3 shows the TEM images of the NiO/SiO<sub>2</sub> and NiO/Al<sub>2</sub>O<sub>3</sub> catalysts after 1 h reaction with methane at 700°C. It was noted that CNTs were grown on both catalysts. The size of CNTs formed

on NiO/SiO<sub>2</sub> was larger than that on NiO/Al<sub>2</sub>O<sub>3</sub>. For NiO/SiO<sub>2</sub> catalyst, only multi-walled CNTs (MWNTs) were formed. Interestingly, a mixture of MWNTs and single-walled CNTs (SWNTs) were grown on NiO/Al<sub>2</sub>O<sub>3</sub> catalyst at 700°C, shown in Fig. 3b-d and indicated by arrow A1,2 and arrow B, respectively. From the TEM analysis, we noticed that the synthesized SWNTs appeared in two forms, i.e. isolated (arrow A1) and bundles (arrow A2). The Raman spectrum (not shown in this paper) shows strong intensity at radial breathing mode (RBM), indicating that the occurrence of SWNTs was dominant. This analysis also reveals that the synthesized SWNTs have a diameter in the range from 0.58 nm to 2.02 nm [8].

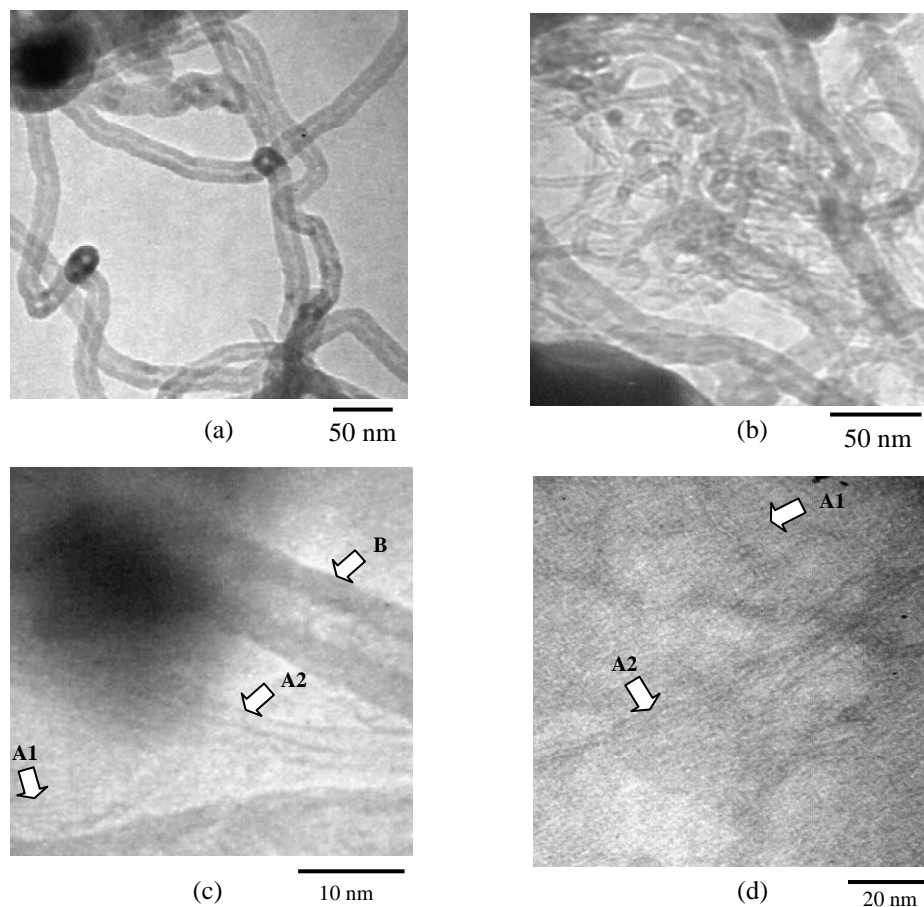


**Fig. 3.** TEM images of CNTs formed on the catalysts after 1hr reaction with methane. (a) NiO/SiO<sub>2</sub> and (b-d) NiO/Al<sub>2</sub>O<sub>3</sub> [8].

To arrive at the understanding why SWNTs were formed on NiO/Al<sub>2</sub>O<sub>3</sub> catalyst, we have to know the nature of the catalyst structure. It is well accepted that the formation of CNTs is governed by the size of the active metal particles. The formation of SWNTs on NiO/Al<sub>2</sub>O<sub>3</sub> catalyst did reveal that very small size of NiO were formed on Al<sub>2</sub>O<sub>3</sub> support and this size was small enough for growing SWNTs. As what we believe, the formation of these ultra-small NiO nanoparticles was mainly induced by the strong MSI effect between the NiO and the Al<sub>2</sub>O<sub>3</sub> support, as previously mentioned. This is because strong MSI allowed high NiO dispersion and prevented NiO from agglomerating and forming larger clusters. Probably, some adjacent NiO particles might combine/sinter during the calcination and reaction stages to form larger NiO particles and these particles led to the formation of MWNTs as observed in the TEM image.

Fig. 4a shows the TEM image of CoO-MoO/Al<sub>2</sub>O<sub>3</sub> catalyst. The dark spots represent the

active metals (indicated by arrows) and the shallow matter is the alumina support. The active metals are the catalyst component subjected to methane decomposition and the growth of CNTs. Fig. 4b shows the TEM image of MWNTs grown on CoO-MoO/Al<sub>2</sub>O<sub>3</sub> catalyst from methane decomposition at 700°C. The high degree of diameter control and uniformity of the synthesized MWNTs can be seen clearly in the TEM image. In addition, the TEM analysis shows that out of total 156 MWNTs measured, more than 98% had diameters ranging from 6 nm to 12 nm. The calculated average diameter and standard deviation were 9.0 nm and 1.4 nm, respectively. This indicates that the formed MWNTs were of higher uniform diameter.

Although many effective ways in producing CNTs with nearly uniform diameters have been suggested in the literature, this study represents a simple and convenient way to achieve this objective. This also reflects a real possibility to produce

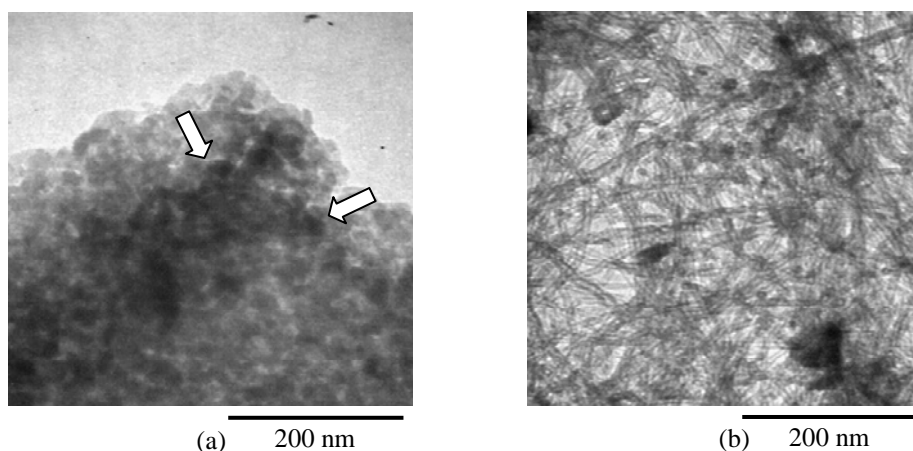


**Fig. 4.** TEM images of (a) CoO-MoO/Al<sub>2</sub>O<sub>3</sub> catalyst, and (b) CNTs formed on the catalyst after 2 hrs methane decomposition [9]

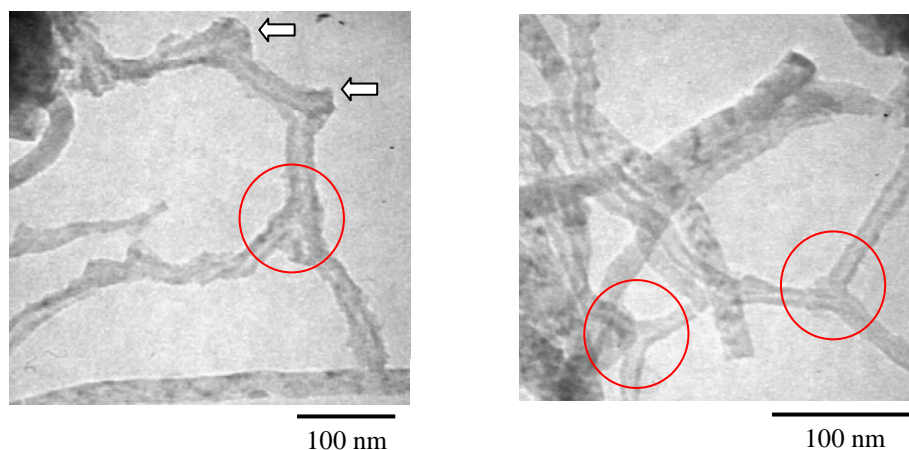


**Fig. 5.** TEM images of Y-junction CNTs grown on NiO-CuO-MoO/SiO<sub>2</sub> catalyst [10].

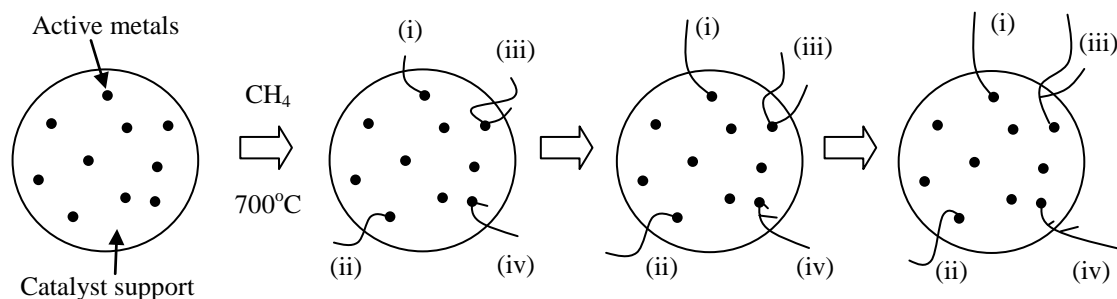
CNTs of uniform diameter by means of a simpler and cheaper approach in the near future, i.e. through controlling the size of the active metals [9].

Fig. 5 shows the TEM images of Y-junction CNTs grown on the complex NiO-CuO-MoO/SiO<sub>2</sub> catalyst from methane decomposition at 700°C. The circles drawn in Fig. 5 indicate the junction part of CNTs. One can notice that three joining tubes branch out from the junction, forming a Y structure. We suggest that Mo is the important factor for the growth of Y-junction CNTs. A small amount of MoO added to NiO-CuO enhances the growth of Y-junction CNTs. A growth model of this special structure is proposed based on the observation of the CNTs' stem and branch. Fig. 6 shows the proposed sequential growth mechanism of straight and Y-junction CNTs [10].

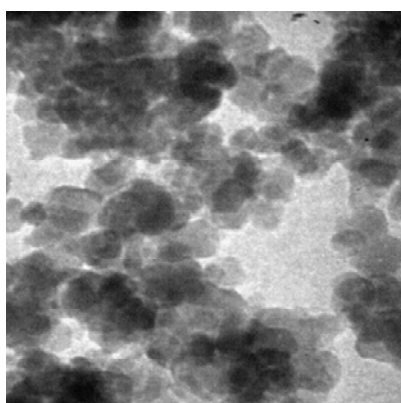
The diagram shown in Fig. 6 illustrates the conditions of the NiO-CuO-MoO/SiO<sub>2</sub> catalyst before

and after CVD reaction. The black dots represent active metals and white circles represent the catalyst support. We expected that not all the added MoO incorporated with NiO-CuO on the SiO<sub>2</sub> support. MoO-free NiO-CuO catalyst would grow straight CNTs, indicated by (i), and (ii) in Fig. 6, whereas MoO-incorporated NiO-CuO led to the growth of CNT stems and branches. Their possible growth mechanism is represented by (iii), and (iv) in Fig. 6. It is likely that the addition of a small amount of MoO to NiO-CuO acts as nucleation sites, seeding the growth of CNT branches. We believe that, after some time, the surface carbons deposited on the active metals will join the graphitic layers for both CNT stems and branches, forming a poorly graphitized junction part. This is evident when most of the junction parts observed under the TEM exhibit poor crystalline wall structure. The continuous growth of a CNT stem forms the Y-

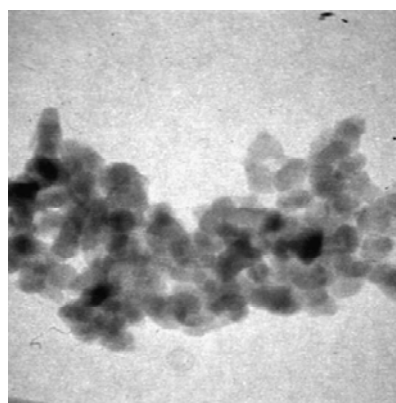




**Fig. 6.** Schematic diagrams showing the proposed sequential growth mechanism of straight (i, ii) and Y-junction (iii, iv) CNTs [10].

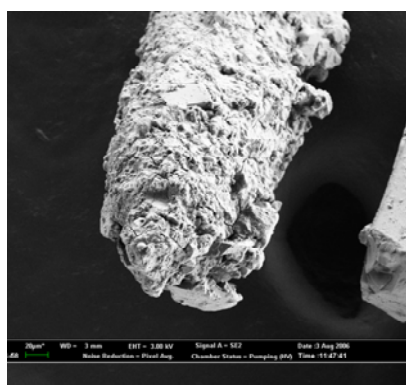


20 nm

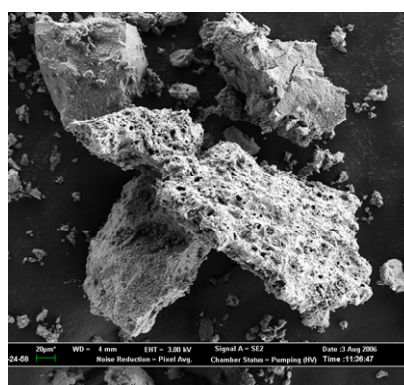


50 nm

**Fig. 7.** TEM images of nanocrystalline  $\text{TiO}_2$  prepared using sol-gel method



20  $\mu\text{m}$



20  $\mu\text{m}$

**Fig. 8.** SEM images of nanocrystalline  $\text{TiO}_2$  using sol-gel method support

junction structure. In the process that follows, other branches could also be formed on the Y-junction CNT stem. The growth mechanism of a second CNT branch is indicated by arrows in Fig. 5 and represented by (iv) in Fig. 6. Y-junction CNTs without short branches, indicated by circles in Fig.

5 were grown on the catalyst, following the mechanism represented by (iii) in Fig. 6.

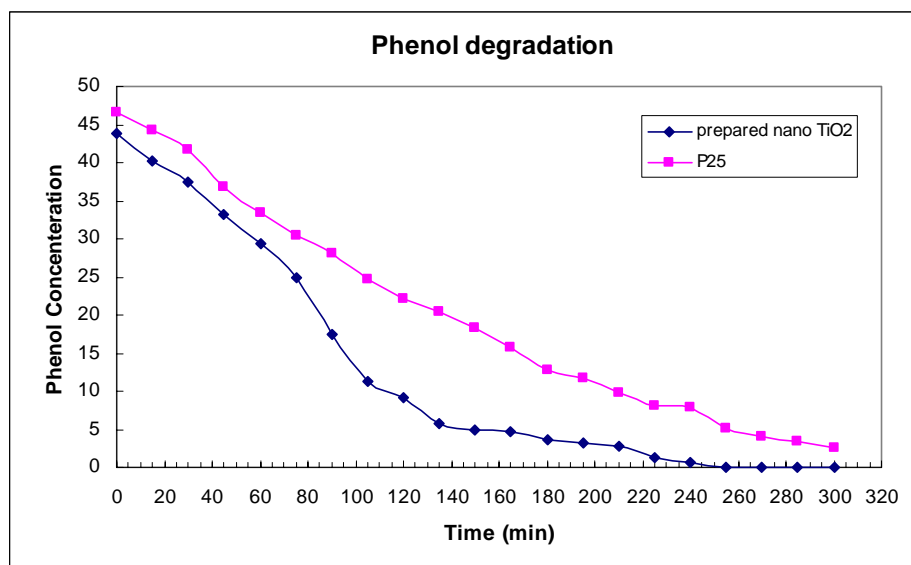


Fig. 9. Photocatalytic degradation of phenol, catalyst 0.6 g, initial phenol concentration of 50 ppm

## 2. Nano TiO<sub>2</sub> for photocatalytic degradation of phenol

Phenol and substituted phenols are widely distributed at low concentration in natural waters, including algal secretion, hydrolyzable tannins and flavanoids and humification processes, and at high concentrations in some industrial wastewater discharge and agricultural activities [11]. Treating phenolic wastewater to harmless level is an arduous process for many biological and chemical processes due to its high solubility and stability in water.

Although a wide range of catalyst has been tested, titania (TiO<sub>2</sub>) seems to be the most widely used catalyst because of its photocatalytic, conservative nature, low cost, low toxicity, corrosion resistant [12] and high stability to light illumination. A way to increase photocatalytic activity is the preparation of a nanostructural to get a high surface area that is directly related with catalytic activity [13]. Moreover, photocatalysis of nanocrystalline TiO<sub>2</sub> has many of advantages on wastewater treatment, such as high catalysis efficiency, energy-saving, non-pollution and can degrade all kinds of organic pollutants from water effectively. All of these merits make photocatalysis of TiO<sub>2</sub> a fine and attractive method in the research of water treatment and it is supposed to be used widely in future.

Fig. 7 shows the TEM images of the prepared nano TiO<sub>2</sub> catalyst. The TEM images data revealed that the catalyst consists of uniform and spherical particles with an average nanoparticles size of

11.50 nm. The SEM images of the catalyst are shown in Fig. 8. It was noted that the catalyst consisting of fine irregular TiO<sub>2</sub> particles agglomerated to form a porous structure.

In order to evaluate photoactivity of prepared nano TiO<sub>2</sub> catalyst, the photocatalytic degradation of phenol in a batch reactor was studied. Fig. 9 shows the photoactivity of the prepared nano TiO<sub>2</sub> catalyst and commercialized TiO<sub>2</sub> powder (Degussa P25). The figure obviously indicates that the phenol concentration decreases with the increase of reaction time. The degradation of phenol using prepared nano TiO<sub>2</sub> is higher than the Degussa P25. It is well known that the higher efficiency of prepared nano TiO<sub>2</sub> is influenced by many factors such as particle size and surface area. In this study, the findings show that the prepared nano TiO<sub>2</sub> has larger surface area, higher porosity and is of smaller particle size than the Degussa P25. This is the reason why the prepared nano TiO<sub>2</sub> is more active than the commercialized TiO<sub>2</sub> powder for photocatalytic degradation of phenol.

## Acknowledgements

The authors would like to acknowledge the financial support provided by the Academic Sciences of Malaysia and the Ministry of Science, Technology and Innovation Malaysia under Scientific Advancement Grant Allocation (SAGA) (Project: A/C No. 6053001), IRPA Long-Term Grant (Project: A/C No. 6012806) and IRPA Short-Term Grant (Project: A/C No. 6035220).

## References

- [1] S.G. Louie, in: M.S. Dresselhaus, G. Dresselhaus, P. Avouris (Eds.), Carbon Nanotubes: Synthesis, Structure, Properties, and Applications, Springer, New York, 2001, pp. 113-145.
- [2] R.H. Baughman, A.A. Zakhidov, W.A. de Heer, Science 297 (2002) 787-792.
- [3] P. Calvert, in: T.W. Ebbesen (Eds.), Carbon Nanotubes: Preparation and Properties, CRC, New York, 1997, pp. 277-292.
- [4] A.G. Mamalis, L.O.G. Vogtländer, A. Markopoulos, Precis. Eng. 28 (2004) 16-30.
- [5] S.P. Chai, S.H.S. Zein, A.R. Mohamed, Diam. & Relat. Mater. (In Press, Accepted Manuscript).
- [6] S.H.S. Zein, A.R. Mohamed, and S.P. Chai, Stud. Surf. Sci. Catal. 159 (2006) 725-728.
- [7] S.P. Chai, S.H.S. Zein, and A.R. Mohamed, Chem. Phys. Lett. 426 (2006) 345-350.
- [8] S.P. Chai, S.H.S. Zein, and A.R. Mohamed. Mater. Lett. (In Press, Corrected Proof).
- [9] S.P. Chai, S.H.S. Zein, and A.R. Mohamed, Carbon (In Press, Accepted Manuscript).
- [10] S.P. Chai, S.H.S. Zein, and A.R. Mohamed, Solid State Commun. 140 (2006) 248-250.
- [11] A. Sobczynski, L. Duczmal, W. Zmudzinski, J. Mol. Catal. A: Chemical 213 (2004) 225-230.
- [12] M. Moonsiri, P. Rangsunvigit, S. Chavadej & E. Gulari, Chem. Eng. J. 97 (2004) 241-248.
- [13] Y. Hwu, Y. D. Yao, N. F. Cheng, C. Y. Tung & H. M. Lin, Nanostructured Materials 9 (1997) 355-358